2017-06

Impacts of Boreal Winter Monsoon Cold Surges and the Interaction with MJO on Southeast Asia Rainfall

Lim, See Yee; Marzin, Charline; Xavier, Prince; Chang, Chih-Pei; Timbal, Bertrand

American Meteorological Society

Lim, See Yee, et al. "Impacts of boreal winter monsoon cold surges and the interaction with MJO on Southeast Asia rainfall." Journal of Climate 30.11 (2017): 4267-4281.
https://hdl.handle.net/10945/60902

Impacts of Boreal Winter Monsoon Cold Surges and the Interaction with MJO on Southeast Asia Rainfall

SEE YEE LIM

Centre for Climate Research Singapore, Meteorological Service Singapore, Singapore

CHARLINE MARZIN AND PRINCE XAVIER

Met Office, Exeter, Devon, United Kingdom, and Centre for Climate Research Singapore, Meteorological Service Singapore, Singapore

CHIH-PEI CHANG

Department of Meteorology, Naval Postgraduate School, Monterey, California, and Department of Atmospheric Sciences, National Taiwan University, Taipei, Taiwan

BERTRAND TIMBAL

Centre for Climate Research Singapore, Meteorological Service Singapore, Singapore

(Manuscript received 27 July 2016, in final form 22 February 2017)

ABSTRACT

TRMM rainfall data from 1998–2012 are used to study the impacts and interactions of cold surges (CSs) and the Madden–Julian oscillation (MJO) on rainfall over Southeast Asia during the boreal winter season from November to February. CSs are identified using a new large-scale index. The frequencies of occurrences of these two large-scale events are comparable (about 20% of the days each), but the spatial pattern of impacts show differences resulting from the interactions of the general flow with the complex orography of the region. The largest impact of CSs occurs in and around the southern South China Sea as a result of increased low-level convergence on the windward side of the terrain and increased shear vorticity off Borneo that enhances the Borneo vortex. The largest impact of the MJO is in the eastern equatorial Indian Ocean, sheltered from CSs by Sumatra. In general CSs are significantly more likely to trigger extreme rainfall. When both systems are present, the rainfall pattern is mainly controlled by the CSs. However, the MJO makes the environment more favorable for convection by moistening the atmosphere and facilitating conditional instability, resulting in a significant increased rainfall response compared to CSs alone. In addition to the interactions of the two systems in convection, this study confirms a previously identified mechanism in which the MJO may reduce CS frequency through opposing dynamic structures.

1. Introduction

During boreal winter, the Asian winter monsoon system dominates the hydrological cycle of Southeast Asia (SEA), which often leads to extreme rainfall events and floods (Johnson and Chang 2007; Wu et al. 2007; Tangang et al. 2008; Pullen et al. 2015). The main remote drivers of the rainfall variability are the northeasterly cold surges (CSs) at the synoptic scale and the Madden–Julian oscillation (MJO) at the intraseasonal scale (Chang et al. 2005a). CSs are spells of strong winds over the South China Sea (SCS) that are associated with southward intrusions of the Siberian high that can result in sustained areas of convection over the Maritime Continent (Ramage 1971; Chang et al. 1979, 2006; Ding 1990; Wu and Chan 1995). The northeasterly flow propagates equatorward and moistens over the South China Sea (Johnson and House 1987). CS events typically occur several times during boreal winter with duration from two days to more than a week. The MJO is an eastward-propagating oscillation that dominates tropical intraseasonal variability (Madden and Julian 1994), with its convectively active phases impacting the rainfall distribution over SEA (Jones et al. 2004;

Corresponding author e-mail: See Yee Lim, lim_see_yee@nea.gov.sg

DOI: 10.1175/JCLI-D-16-0546.1

Xavier et al. 2014). These large-scale phenomena interact with the complex orography and local circulations such as the Borneo vortex and often produce strong convection with its distribution depending on the specifics of the interactions (Chang et al. 2005a, 2016).

The impacts of the intraseasonal and synoptic variability and their interactions with convection in the western Maritime Continent during boreal winter have been studied by Chang et al. (2005a), using a rainfall proxy: a convection index based on a 21-yr (1980–2001) satellite blackbody temperature data for December–February (DJF). They found that the convection is most active during CSs and over the windward side of the coastal mountains downstream of the surges, where strong wind–terrain interaction takes place. The presence of the Borneo vortex complicates this convection pattern because its variation changes the wind circulation around the southern SCS. The eastward propagation of the MJO from the Indian Ocean gives rise to active or suppressed convection over the area depending on the specific MJO phase, but during CS the active convection phase of MJO does not alter the pattern of convection, which is still dominated by the wind–terrain interaction from the CSs. They also found a reduction in the frequency of CSs during one-half of the MJO cycle: the suppressed phase and the transition from suppressed to active phase over the broad Maritime Continent domain implying a dynamical interaction with anomalous southerly and southwesterly winds linked to the MJO phases that partially counter the main northeasterly monsoon winds over the northern SCS.

An important limitation of the Chang et al. (2005a) study is to rely on a proxy of the convection. Although they deduced the inhibition of cold surges during certain phases of the MJO, they did not analyze the convection associated with the MJO outside of the immediate land areas surrounding the South China Sea. Furthermore, there were significant difficulties in using their proxy data to study the interaction mechanisms between cold surges and MJO in the most important fields: those of the deep convection and heavy rainfall. Thus, some key processes of the coupled dynamic and thermodynamic interactions could not be elucidated. Here we are proposing to use the Tropical Rainfall Measuring Mission (TRMM; Huffman et al. 2007), which provides a continuous rainfall dataset covering the period from 1998 onward and allows direct study on the rainfall impacts of CSs and MJO that provide forcing from outside of the region. The quasistationary Borneo vortex that was studied by Chang et al. (2005a) is a local system that interacts with both cold surges and MJO and always has strong effects on rainfall. Its explicit impacts will be left to future study focusing on the local signature of CS. The rainfall data are also better in revealing important mesoscale structures that are often masked by the large-scale outgoing longwave radiation pattern represented by the blackbody temperature index. It also provides the opportunity to extend the study period (1980–2001) of Chang et al. (2005a) offering a possibility to assess a potential multidecadal signal (because of either naturally occurring variability or forced anthropogenic climate change; Meteorological Service Singapore 2015), if any.

Section 2 describes the data and methods including the definition of two CS indices, one based on low-level wind speed and mean sea level pressure (MSLP) and the other based on low-level wind speed only. Section 3 presents the mean climatology of the NDJF season and both CSs and MJO large-scale events in the region. Section 4 discusses the joint impacts of MJO and CSs on mean and extreme rainfall, their seasonality, and the dynamic interactions between the two large-scale systems. Concluding remarks from this study in light of earlier studies (e.g., Chang et al. 2005a) and potential future work are given in section 5.

2. Data and methods

Daily datasets (precipitation, 850-hPa winds, MSLP, SST, and MJO index) for November, December, January, and February (NDJF) from 1998 to 2012 covering the SEA region are used in this study. The month November was included in the boreal winter season on the grounds that the CS events could first be observed to affect the region around late October or early November (Wongsaming and Exell 2011; Moten et al. 2014). Also, November is the second wettest month over the region after December (see section 2 and Fig. 2) and is a month when operational forecasters begin to monitor cold surges. The daily mean precipitation data are obtained from the TRMM 3B42 dataset with a resolution of 0.25°× 0.25°. The daily MSLP and 850-hPa winds are obtained from ERA-Interim (ERA-I) at 1° × 1° and 0.5° × 0.5° resolutions, respectively (Dee et al. 2011), and the daily mean SST data are from the NOAA high-resolution blended analysis at 0.25° × 0.25° resolution (Reynolds et al. 2007).

These daily data are analyzed using CS- and MJO-based indices. To do so, the real-time multivariate MJO index (RMM; Wheeler and Hendon 2004) is used to identify MJO amplitudes and phases. We focus on active MJO phases 2, 3, and 4 that correspond to enhanced convection in the SEA region (Xavier et al. 2014). Several indices of CS have been defined since the winter monsoon experiment (e.g., Chang et al. 1979; Chu and Park 1984), most of which are based on a low-level meridional wind component averaged over a specific area in the northern or middle SCS. However, a strong low-level northerly wind could be induced by local tropical circulations, rather than cold surges forced by the southward extension

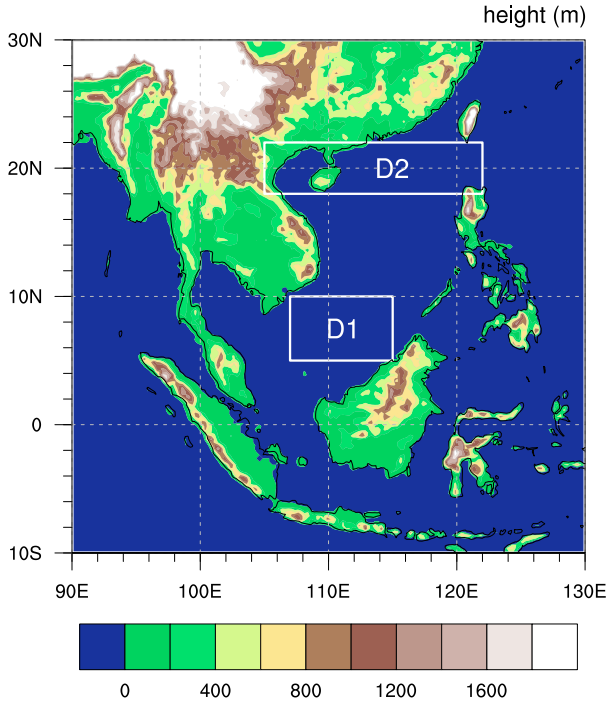

FIG. 1. Topography map (m) for Southeast Asia. The cold surge indices are defined in the two rectangular boxes: northerly or northeasterly wind speed in domain D1 (5°–10°N, 107°–115°E) and MSLP in domain D2 (18°–22°N, 105°–122°E).

of the Siberian high (Ding 1990). Therefore, we have combined both a wind index and a pressure index in this study. The wind index is computed at 850 hPa over domain D1: 5°–10°N, 107°–115°E (Fig. 1), as per Chang et al. (2005a). The MSLP index is computed over domain D2: 18°–22°N, 105°–122°E (Fig. 1). The two indices are significantly correlated [at the 95% level, correlation coefficient (cc) is 0.51], but that correlation explains only 25% of the covariance of the two indices.

For a CS event to be counted, wind equaling 0.75 standard deviation (2.78 m s^{-1}) above the long-term mean (7.56 m s^{-1}), or 9.65 m s^{-1}, is required. Such a definition relative to mean climatology is preferred to facilitate future investigations of CS representation in climate models. A surge day is flagged when the wind direction is northerly or northeasterly with a speed above the threshold, providing MSLP is above 1020 hPa anywhere within the domain D2. This threshold is commonly used by operational forecasters in the region to monitor CSs.

A CS is identified when both the wind and the MSLP thresholds are satisfied, with at least two days within a 4-day window meeting the criteria in Table 1. To facilitate the comparison with previous studies using an index based on low-level winds only, another index is investigated for completeness. In the absence of the MSLP criteria, a wind-only surge (w-S) event is defined based on days that meet only the wind index criteria. Table 2 summarizes all the terminology used in regard of CS and MJO states.

3. CS and MJO climatologies

The annual cycle of monthly mean rainfall over the Maritime Continent averaged from 1998 to 2012 (Fig. 2) shows that February is the driest boreal winter monsoon month corresponding to the wet monsoon advance southward of the equator (Ramage 1971; Chang et al. 2005a), while the other three months are the wettest of the year, underlining the importance of the northeast (NE) monsoon in terms of annual total rainfall for the region. In February most heavy rainfall events tend to occur around western Java and the southeastern Philippines. Corresponding NDJF seasonal mean rainfall, 850-hPa winds, SST, and MSLP over the SEA region were averaged for 1998–2012 (Figs. 3a–c). As a result of the interaction of the large-scale circulation and the complex local terrain, the overall boreal winter and summer monsoon regimes are partitioned along the equator but with an asymmetry such that the boreal winter wet regime intrudes northward where wind–terrain interaction produces rainfall in winter (Chang et al. 2005b). Most of the

TABLE 1. Summary of cold surge indices based on the area-average 850-hPa winds and maximum MSLP over the domain indicated. Here u and v are zonal and meridional winds, respectively, $\overline{V}$ denotes long-term average, and σ_V the standard deviation of the meridional wind speed V.

Variable	Criteria		Lat	Lon
850 hPa wind averaged over domain D1	Calm to easterly wind	$u \le 0$ m s^{-1}	5°–10°N	107°–115°E
	Northerly wind	$v < 0$ m s^{-1}		
	Normalized wind speed at least 0.75 standard deviations above long-term mean	$\frac{V-\overline{V}}{\sigma_V} \ge 0.75$		
Max MSLP in domain D2	MSLP at least 1020 hPa	MSLP $\ge$ 1020 hPa	18°–22°N	105°–122°E

A single event includes a minimum duration of 2 days with a maximum allowable gap of 2 days between cold surge days.

TABLE 2. Definition of terms used to characterize cold surge and MJO days and events.

Event	Definition
CS	Full CS events meeting both the wind and MSLP index criteria (total 360 days).
w-S	Surge days that only meet the wind index criteria but not the MSLP criteria (total 78 days). They can occur in connection with either a full CS event or a CS event that satisfies only the wind index criteria but not the MSLP criteria.
nCS	All days with no CSs.
MJO	All active MJO in phases 2–4 [amplitude ≥ 1; based on MJO index defined by Wheeler and Hendon (2004)].
nMJO	All days with no active MJO in phases 2–4 (this includes MJO days in phases 1 and 5–8).
CS+nMJO	Days in NDJF with only CSs and no MJO as defined above.
MJO+nCS	Days in NDJF with only MJO events.

northern SEA region experiences dry weather, especially over the region to the north of 10°N and west of the Philippines (Fig. 3a). Higher rainfall is observed over the ocean west of Sumatra, northern Borneo, and the eastern Philippines. A strong low-level northeasterly wind belt oriented northeast–southwest in the southern SCS turns counterclockwise to northerly as the winds cross the equator and becomes westerly south of the equator (Fig. 3b). This low-level jet-like configuration results from the combined influences of the orientation and narrowing of the SCS toward the equator and the effects of a dynamic response to periodic midlatitude pressure forcing that behave like a dispersive group of equatorial Rossby meridional modes under surge conditions (Chang et al. 2016). The southward intrusion of the higher MSLP and associated colder SST from northern SEA are conspicuous (Fig. 3c).

Over the study period (1998–2012), around 25% of the days meet both the wind and the MSLP CS index thresholds during DJF (down to 20% when November is included; Table 3). Chang et al. (2005a) obtained 20% in their study period 1980–2001 for DJF. The small increase may not be meaningful as the two studies used very different thresholds; for example, Chang et al. (2005a) only relied on a wind index without considering MSLP threshold and used a wind threshold of $8\,\mathrm{m\,s^{-1}}$ but at a lower level (925 hPa) and relying on a coarser reanalysis. On average, 4.7 cold surge events occurred each year with a mean duration of around 5.1 days. The numbers are higher than those reported by operational weather services in Singapore and Malaysia, both of which experienced an average of 2–4 CS events yearly with each lasting around 1–5 days (see Meteorological Service Singapore communication on CSs available online under the Monsoon Surge dropdown at http://www.weather.gov.sg/learn_weather_systems/). This is most likely due to a difference of opinion as operational services focus on stronger cases and localized impact that have a high probability to be associated with significant weather events. Table 3 summarizes numbers across the different studies while the full CS statistics from this study are provided in Table 4.

The composite fields of all full surge days (Figs. 3d–f), to a large degree, appear to be an enhanced version of the seasonal mean fields as outlined by the composite anomalous fields (Figs. 3g–i). During CS days, higher rainfall occurs over the southeastern Philippines, north and west of Borneo, the southeastern Malay Peninsula, southeastern Sumatra, and Karimata Strait and Java Sea (Fig. 3g). Compared to previous studies (Chang et al. 2005a,b), the TRMM rainfall shows clearly that the highest rainfall intensity is on the windward side of the terrain. The concentration of heavy rain near the western coast of Borneo where the northeasterly surge winds are parallel to the coastline is associated with enhanced shear vorticity and the strengthening of the Borneo vortex during surges (Chang et al. 2005a). Negative

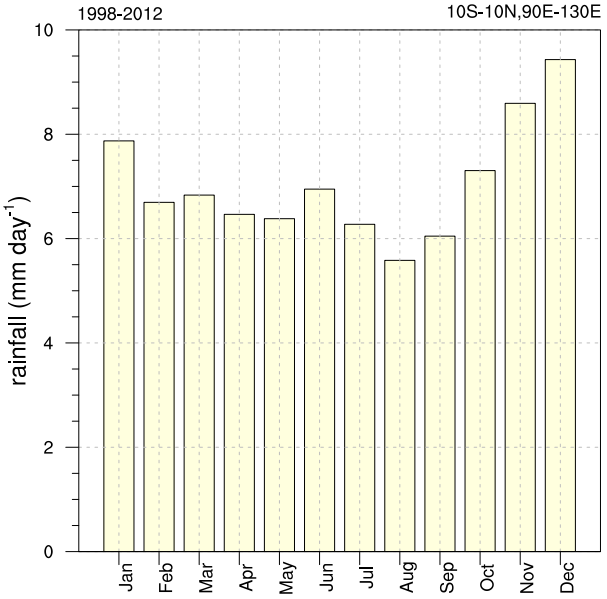

FIG. 2. The 15-yr (1998–2012) monthly mean rainfall ($\mathrm{mm\,day^{-1}}$) averaged over the Maritime Continent region (10°S–10°N, 90°–130°E).

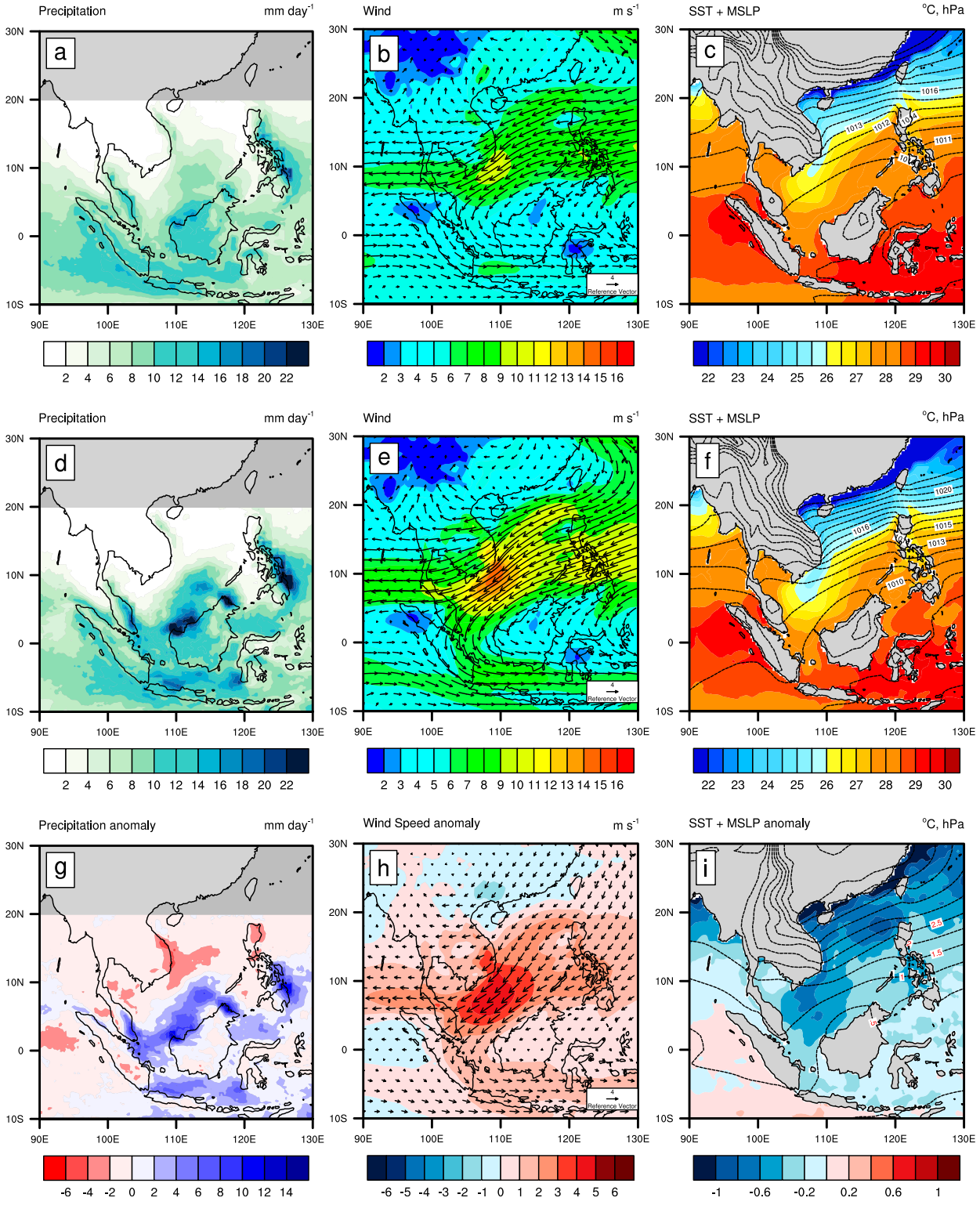

FIG. 3. The 15-yr (1998–2012) NDJF mean for (a) precipitation (mm day^{-1}), (b) wind speed (shaded and vectors; m s^{-1}), and (c) MSLP (contours; hPa) with SST (shaded; °C); the composites of CS days for (d) rainfall (mm day^{-1}), (e) 850-hPa wind speed (shaded and vectors; m s^{-1}), and (f) MSLP (contours; hPa) and SST (shaded; °C). (g)–(i) The anomalies between (a)–(c) and (d)–(f), respectively.

TABLE 3. Distribution of the average CS occurrences, events, and duration during the NE monsoon season from the current study, Chang et al. (2005a), and Singapore weather forecasting guidelines.

Source	Time period	CS occurrence (days)					Average CS event (episodes)	Average CS duration (days)
		Nov	Dec	Jan	Feb	DJF		
Current study	NDJF 1998–2012	1.1	7.0	11.1	4.9	23.0	4.7	5.1
Chang et al. (2005a)	DJF 1980–2001	—	9.9	5.7	2.5	18.1	—	—
Singapore weather forecasting guidelines	DJFM	—	—	—	—	—	2–4	1–5

rainfall anomalies are limited primarily to the east of Vietnam, a consequence of the strengthening of the Borneo vortex depleting water vapor farther north by transport around the Borneo vortex to support the heavy rainfall anomalies farther south. An indication of negative rainfall anomalies observed to the west of Sumatra offers the clue of a forced downward motion on the lee side of the mountain, which is not discernible in Chang et al.'s (2005a) convective index data. The strengthening of the surge winds is general over the region but strongest along the southern SCS area (Fig. 3h), a direct consequence of the intrusion of higher MSLP southward into the SEA region (Fig. 3i).

With wind-only surges, the percentage of CS days increased to about 25% of the days in NDJF. There are 78 w-S days (Table 4). Wind and rainfall composites for wind-only CS days are displayed in Fig. 4 alongside anomalies computed from the composite based on 360 full CS days. Wind-only surge composites have weaker northeasterlies indicating weaker CS events and consequently weaker rainfall anomalies in areas where the wind–terrain interaction is strongest (e.g., off the southeast coast of the Philippines, the southeastern Malay Peninsula, Karimata Strait and Java Sea, and northern Borneo). An opposite signal, with positive rainfall anomalies, is seen southwest of Sumatra and off the northwest coast of Borneo. All anomalies are consistent with a weaker impact of the CS winds on areas where the impact enhances rainfall through wind–terrain interaction, which is a clear indication that once a full surge develops, regional rainfall effect is not very dependent on the MSLP threshold being met. Nevertheless, the MSLP index provides additional information to differentiate the strong and weak surge events over the common practice of using wind speed only. Indeed, the average of the wind speed index (11.2 m s^{-1}) is higher for the full surge events than that of the wind-only events (10.5 m s^{-1}), but the range of the wind-only events (9.8–11.4 m s^{-1}) is within the range of the full surge events (9.5–13.4 m s^{-1}). It confirms the usefulness of combining the wind and MSLP indices, which are only modestly correlated. The MSLP threshold also ensures that few days with local tropical circulation resulting in strong northerlies are avoided and represents another useful indicator of the large-scale circulation favoring cold surges to be used in modeling studies. Hereafter, the CS index is used to further analyze the impact of cold surges on rainfall and its interplay with the MJO.

RMM phases 2–4 with normalized amplitude greater than 1 (Wheeler and Hendon 2004) correspond to more active convection over the Maritime Continent region during boreal winter than in other seasons (Xavier et al. 2014) and are selected to analyze the impact of the MJO. Hereafter, unless otherwise specified, MJO refers to only the days of RMM phases 2–4 (Table 5). Over the 15-yr period, the total number of MJO days is 415, or about 23% of the total days. Thus, the frequency of MJO is comparable to that of the surge days of 20%–25%. The composites of wind and rainfall anomalies for the eight RMM phases when RMM ≥ 1 (Fig. 5) show that over the northern SCS southerly wind anomalies up to 1 m s^{-1} start at phase 1 and evolve into expansive southwesterly anomalies with magnitudes up to 2 m s^{-1} in phases 2 and 3. In phase 4 the anomalies become northeasterly and persist through phases 5 and 6, with amplitudes around 1 m s^{-1}. The amplitude of wind anomalies in all phases are small compared to the anomalies because of CSs.

The anomalies in the equatorial region are correlated to those in the northern SCS in that equatorial westerlies are observed in phases 1–3, and equatorial easterlies are observed in phases 4–7. The resulting circulation pattern is consistent with the evolution of the active and suppressed locations represented by the rainfall anomalies. The most distinctive manifestation of this relationship is shown in phase 5, where strong positive rainfall anomalies are observed in the center of a synoptic vortex centered at 10°N in the middle of the SCS. This is linked to the strong wind

TABLE 4. Statistics of CSs and w-S during NDJF of 1998–2012.

Total CS events	70 episodes
Average CS events per season	4.7 episodes
Total CS days	360 days
Average CS duration	5.1 days
Frequency of CS days in NDJF	20%
w-S events	10 episodes
w-S days	78 days

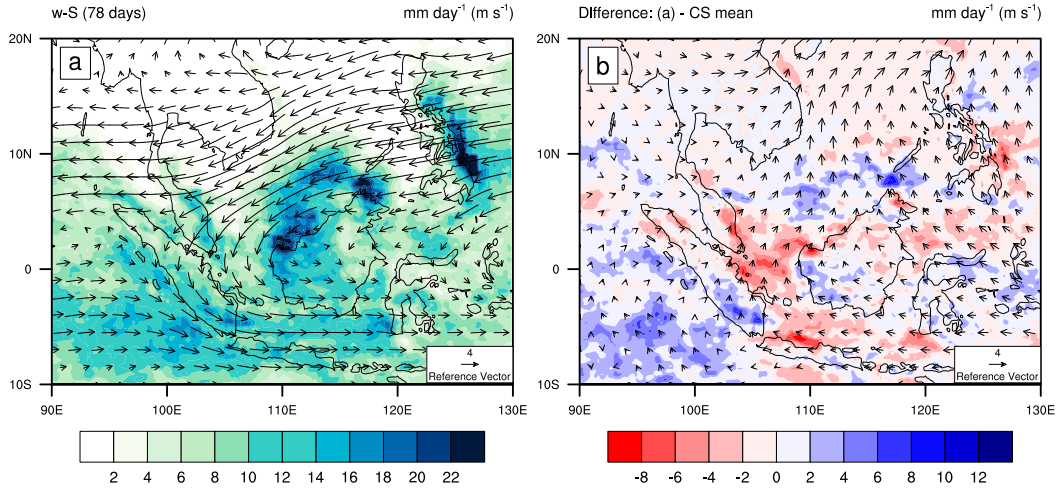

FIG. 4. (a) Mean wind and precipitation composite for all 78 w-S days and (b) the anomalies from the 360 full CS days (shown in Fig. 3).

anomalies along the coasts of central Vietnam and eastern Philippines, where the wind–terrain interaction is the strongest. For the three phases defined as an active MJO over SEA, southeasterlies (in phases 2 and 3) turn into southwesterlies (in phase 4) across the southern SCS, while there are southwesterlies in the northern SCS. So during the SEA active MJO period, despite similarity in rainfall anomalies, the circulation anomalies resulting from CSs and MJO are basically opposite, in agreement with Chang et al. (2005a), although the magnitudes of the wind anomalies are smaller for the MJO than for CSs.

4. The interplay between the MJO and CS

a. Mean rainfall response

Anomalies of rainfall and 850-hPa winds for CS and MJO days side by side, as well as for days when both are present (Fig. 6), outline the similarities and differences of the impact of these two large-scale events and how they interact. The CS rainfall anomalies discussed earlier can be summarized in an increase of rainfall across the southern SCS along an asymmetric "V" shape with a short left arm and a long right arm, or SCS "check mark pattern." Meanwhile, the effect of an intensified Borneo vortex resulting from the enhanced shear vorticity leads to increased rainfall northwest of Borneo and decreased rainfall off the eastern Vietnam coast, or a "parallel dipole pattern." South of the equator, after the wind turns counterclockwise, the wind–terrain interaction gives rise to positive rainfall anomalies over the Java Sea. Overall the following areas are the most strongly impacted by CSs: 1) the southeastern Philippines, 2) the SCS check mark pattern coupled with the Borneo vortex parallel dipole pattern, and 3) the Java Sea, all of which experience strong wind–terrain interactions.

The MJO rainfall anomalies have some similarities in some places (e.g., increased rainfall in the SCS), while being almost opposite of the CS anomalies in others (e.g., west of Sumatra and east of the Philippines). When both events concurred, the rainfall anomalies (Fig. 6c)

TABLE 5. Frequency of CSs during MJO phases 2–4 and phases 5–8 and 1 for all MJO days, RMM ≥ 1 day, and RMM < 1 day.

Surge selection		Wind and MSLP thresholds		MSLP threshold not used	
	MJO days	Surge days	Frequency	Surge days	Frequency
All RMM					
Phases 2–4	663	116	17.5%	153	23.1%
Phases 5–8 and 1	1141	244	21.4%	285	25.0%
RMM ≥ 1					
Phases 2–4	415	75	18.1%	102	24.6%
Phases 5–8 and 1	716	173	24.2%	197	27.5%
RMM < 1					
Phases 2–4	248	41	16.5%	51	20.6%
Phases 5–8 and 1	425	71	16.7%	88	20.7%

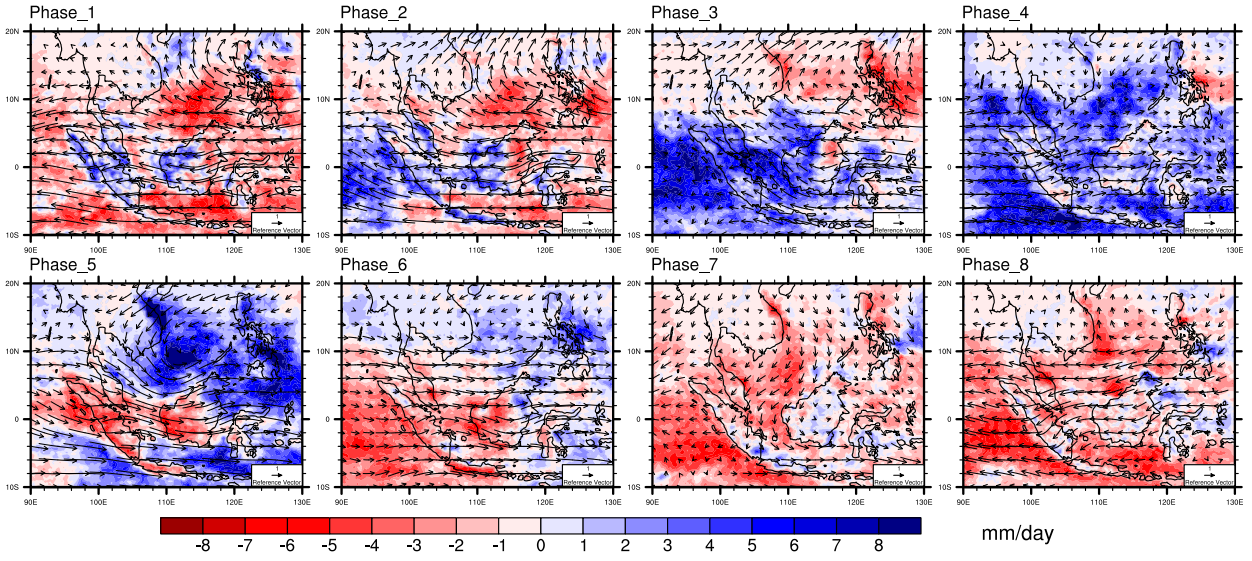

FIG. 5. Wind (vectors; m s^{-1}) and rainfall anomalies for the eight MJO phases with RMM ≥ 1.

contain features of both patterns; not surprisingly the strongest anomalies are located around the southern SCS where both large-scale events contributed individually in that direction and also east of the Philippines where the CS dominates. Already it is obvious that some nonlinearities are at play as the map of the combined effect does not resemble a straight addition of the two individual impacts.

This is further investigated displaying the ratio of rainfall intensity versus long-term mean for CS and MJO days and days when both CSs and MJO are present (Fig. 7a–c). In addition, a straight multiplication of the two individual ratios is used to estimate what to expect if no nonlinearity were involved (Fig. 7d), and the difference with the combined effect (Fig. 7e) provides insight on the nonlinearities between the two large-scale events. In general, both the CS and MJO cases see rainfall intensity in excess of 50% above the mean in places where they dominate. For CSs this is concentrated in the southern SCS check mark pattern and in smaller areas across the Java Sea and east of the Philippines. For MJO the largest ratio is mainly over the Indian Ocean west of Sumatra and over central Indochina north of 15°N with a small signature located at the bottom of the SCS, in the vicinity of Singapore. Both systems also raise the rainfall intensity modestly over a large domain in the equatorial region south of 10°N, with CSs affecting mainly the southeastern part of the domain that is either directly under or downstream of the cold surge and cross-equatorial winds, whereas the MJO affects mainly the western part of the domain and the southern equatorial region, where the MJO is known to maintain its amplitude in its eastward propagation across the Maritime Continent. Overall, CSs and the MJO each contribute up to 40% of the total NDJF rainfall locally (not shown).

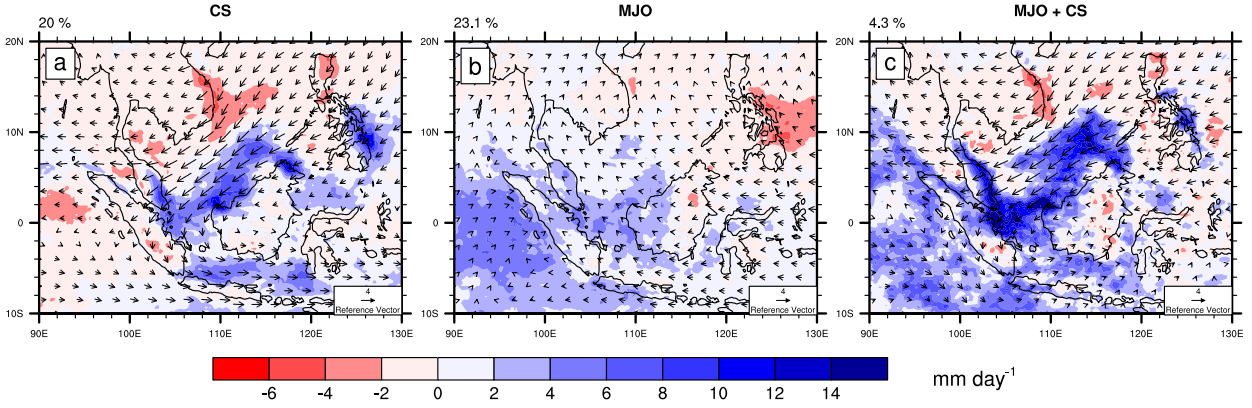

FIG. 6. Composite of rainfall (shaded; mm day^{-1}) and 850-hPa wind speed anomalies (vectors; m s^{-1}) during NDJF for (a) CS, (b) MJO, and (c) CS+MJO events. The percentage of occurrence for each relative to total NDJF days is given at the top left of each panel.

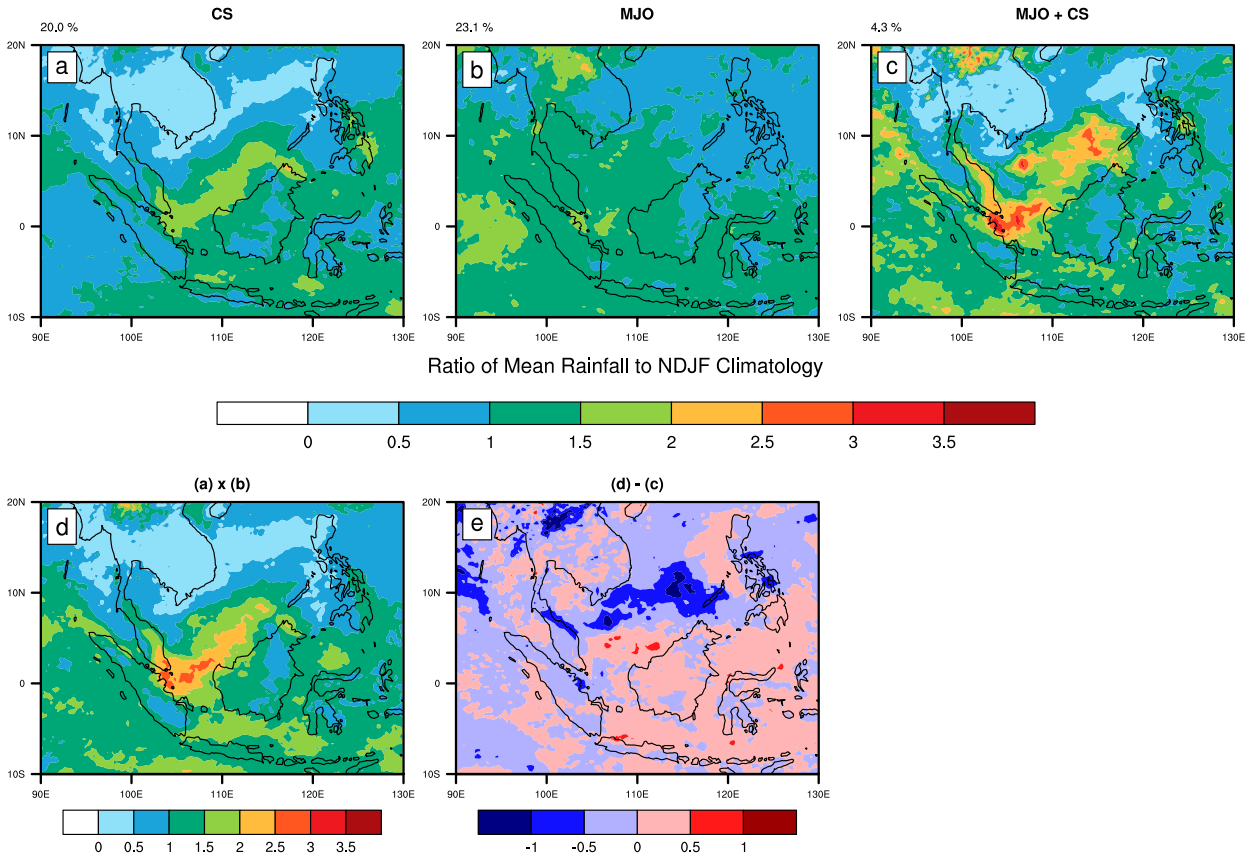

FIG. 7. (a)–(c) As in Fig. 6, but for the ratio of mean rainfall intensity to climatology. (d) The direct multiplication of (a) and (b); (e) the difference between (d) and (c).

Instances of joint MJO and CSs are rare (4% of the days), but in those rare occasions, the rainfall intensity can triple the long-term mean in the southern SCS (Fig. 7c)—significantly above the effect of each occurring either alone or linearly combined (Fig. 7d). Across the SCS, the pattern for joint events resembles more closely the CS pattern (the correlation coefficient between the two maps is 0.43) than the MJO pattern (cc = 0.15). Thus, the distribution of impacts on rainfall in the region when both events occurred is strongly controlled by the CS events (as noted by Chang et al. 2005a). But the nonlinearity of the interaction is worth noting, and the additional effect (Fig. 7e) implies that, when the MJO is present, the arrival of the eastward-propagating MJO in the western part of the domain induces an overall increase of water vapor covering most of the southern SCS, providing a favorable environment for convection. The mechanism for this may be analogous to the ''vanguard effect'' ahead of the MJO active regime that increases the diurnal cycle convection over the Maritime Continent (Peatman et al. 2014). In the present case the moistening effect is stronger because the MJO active regime has reached the CS convection region.

b. *Impact on extreme rainfall*

The active MJO phase is known to relate to the intensification of extreme rainfall over the Maritime Continent (Xavier et al. 2014). PDFs for all rainfall days ($\geq$1 mm day^{-1}) clustered in six categories representing various combinations of the presence and absence of CSs and the MJO over the Maritime Continent are shown in Fig. 8, and extreme rainfall is defined as that in excess of the 95th-percentile rainfall of all rainfall days (the top of the box-and-whisker plot for NDJF). The highest chance of reaching this threshold is when CS and MJO days coincide (MJO+CS), followed by all CS days and all active MJO days, with little difference whether the CS and MJO coincidence days are removed from the last two categories. In contrast the days without either event (nMJO+nCS) have the least chance of extreme rainfall. The PDFs for each of the four individual months (not shown) are similar.

The spatial patterns of the increase of probability of rainfall exceeding the NDJF 95th percentile (Fig. 9) show

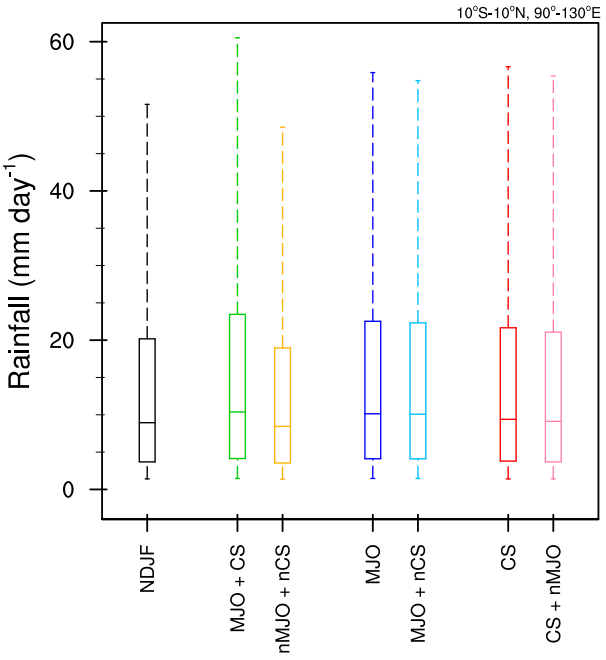

FIG. 8. Box-and-whisker plots showing the 25th, 50th, 75th, and 95th percentiles of rainfall (mm day^{-1}) averaged over the region 10°S–10°N, 90°–130°E for NDJF, MJO+CS, nMJO+nCS, MJO, MJO+nCS, CS, and CS+nMJO days. Values are computed from days with at least 1 mm of rainfall.

the area of extreme rainfall favored by CSs, the MJO, and a combination of both. Note that, to help with the interpretation of the figure, the areas with decreasing probability have been masked out as the changes are insignificant. In general, the changes in extreme rainfall probability share a similar spatial distribution with the positive rainfall anomalies in Fig. 6. Higher chances of exceeding the extreme rainfall threshold are observed over the respective parts of the Maritime Continent where CS or MJO impacts rainfall the most. During CS days the probability of exceeding the NDJF threshold is increased by 20% (and up to 80% locally) over the coastal regions south of the Malay Peninsula, north and west of Borneo, and southeast of the Philippines (Fig. 9a), but the southern tip of the SCS check mark pattern seen on mean rainfall maps (Fig. 6) is broken for extreme rainfall with little signal in the Karimata Strait. An illustration of this was the very severe flood event from the winter of 2006/07 over the southern Malay Peninsula that was associated with a cold surge and an active phase of the MJO (Tangang et al. 2008). During MJO days the magnitude of increase in extreme rainfall rarely exceeds 20%–30% and is primarily over the ocean west of Sumatra and parts of Borneo (Fig. 9b). While there is hardly any overlap between the influence of both large-scale events on extreme rainfall when occurring separately, in the rare instances when the MJO and CSs coincide, the probability of extreme rainfall increases markedly and over extensive parts of the Maritime Continent region (Fig. 9c), covering the area of enhanced extreme rainfall resulting from either CSs or the MJO alone but extending farther; overall the joint effect is more aligned with the CS impact [cc between the two maps (Figs. 9a,c) is 0.24, compared with cc = 0.07 between MJO and combined effects (Figs. 9b,c)]. The combined impact, with up to doubling or more the probability of extreme rainfall, is most prominent around the southern tip of the SCS. That corresponds to the area where the combined effect for the mean rainfall was also noted to be enhanced compared to the separate influences alone, thus suggesting that a large part of the additional effect from nonlinearity and interplay between the two large-scale influences is importantly experienced through an effect on extreme rainfall. This may be indicative of the importance of the moistening effect of the arriving MJO that enhances the convective available potential energy, such that the conditional instability is significantly enhanced.

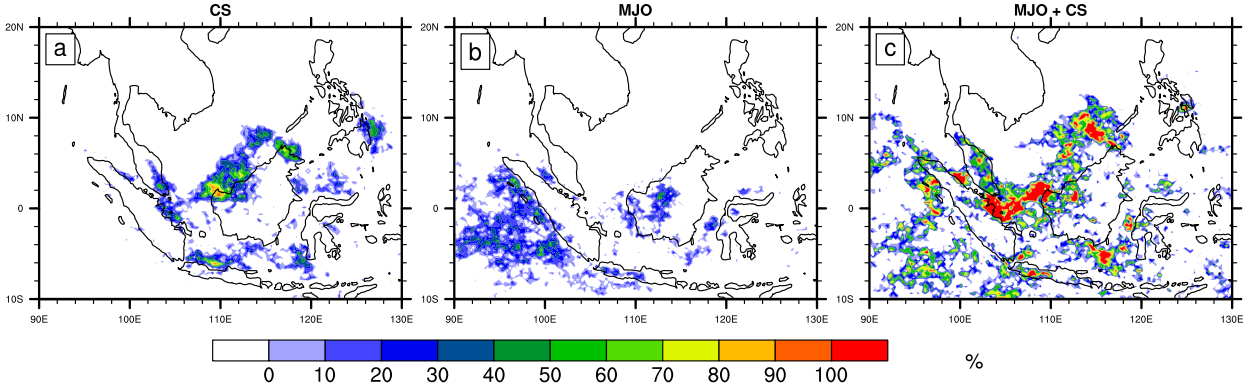

FIG. 9. As in Fig. 6, but for the percentage change in probability of extreme rainfall (above the 95th percentile). Values are computed from days with at least 1 mm of rainfall.

c. *Evolution of the impacts during the northeast monsoon*

In this study, it was considered useful to extend the analysis to the month of November in addition to boreal winter, in contrast to many prior studies (e.g., Chang et al. 2005a). A month-by-month analysis of the monthly rainfall and wind speed anomalies of CSs, MJO, and MJO+CS days relative to the long-term mean rainfall (Fig. 10) depicts how these influences evolved during the NE monsoon season. The wind and rainfall anomalies associated with CSs, both without and with the MJO, are strongest during November (Figs. 10a and 10c, respectively), clearly confirming the importance of including November in studying the northeast monsoon. Early in the season, the mean monsoon flow is not fully established, and hence the monsoon is primarily experienced through the burst associated with CS, therefore giving the largest flow anomalies over the northern China Sea of all months. Interestingly, it also corresponds to a time where flow from the MJO and associated anomalies are more benign compared to later in the season; consequently, the CS signals dominate those of the MJO when both are present (Fig. 10c).

The strongest rainfall anomaly signals are found in locations on the windward side, such as the vicinity of the eastern Philippines and Malay Peninsula (i.e., the left arm of the check mark pattern), the parallel dipole pattern between the south and east coast of Vietnam, and the northwest coast of Borneo. During November the Siberian high does not frequently extend deeply into the subtropics, and low-level winds to the south are more easterly than other winter months for both the monthly mean wind and the surge wind, explaining why the parallel dipole pattern is more zonally oriented. Since surges strengthen the Borneo vortex through a strengthening of the shear vorticity and the easterly wind component provides a stronger westward advection of the vortex, the positive rainfall anomalies of this parallel pattern may be at least in part related to the enhanced Borneo vortex activity.

As the season evolves, three general tendencies can be observed. The first two are a southward extension of the surge wind and a decrease of rainfall anomalies over the SCS. The southward extension of the wind anomalies follows the southward extension trend of the seasonal march of the monthly mean wind (Chang et al. 2005a). There is a weakening of the surge winds in the SCS from December to January (Figs. 10d,g) and associated weakening of the positive rainfall anomalies downstream in the check mark pattern area and the Java Sea. Finally, in February the northeasterly surge winds upstream strengthen and reach deeper into the southern tropics (Fig. 10j), and the rainfall anomalies cease to affect the southern tip of the Malay Peninsula and Singapore. Outside of the SCS, all positive rainfall anomalies in regions of strong wind–terrain interaction, including the southeastern Philippines and northeastern Borneo and the Java Sea, increase in February. On the other hand, rainfall anomalies in the southern SCS decrease, which may be related to two developments of the seasonal march. First, after being exposed to the cold and dry northeast monsoon air for several months, the northern and central SCS SST reaches minimum value in the annual cycle (see http://envf.ust.hk/satop/south-china-sea.html). Second, the geography of Asia, Australia, and the Maritime Continent creates a tendency of low-level divergence over the region from boreal winter to spring. This tendency that inhibits convection is the result of the redistribution of mass between land and ocean areas because of the different thermal memories (Chang et al. 2005b). With less convection the strong surge wind streams through southwestward and crosses the equator to turn counterclockwise in the Java Sea. This wind anomaly pattern is consistent with the interpretation of the dispersion of the meridional modes of the equatorial Rossby waves described in Chang et al. (2016).

Another evolution during the season is the southward migration of the path of the MJO, consistent with the drying trend across the region as the monsoon front penetrates farther south. This migration causes the MJO-induced wet anomaly to weaken and to withdraw southward from December to February (Figs. 10e,h,k). On the other hand, the dry anomaly southeast of the Philippines that intensifies from November to January appears to weaken slightly in February, although overall it remains a robust feature of the MJO composite.

The robust opposite relationship between the CS and MJO composites east of the Philippines can be explained in terms of the northwest–southeast orientation of the coast line, almost perpendicular to the onshore northeasterly surge winds during CS ensuring positive rainfall anomalies. Meanwhile, for MJO days this is the region to the northeast of the active convection region and northwest of the suppressed region, and the Rossby wave response (Matsuno 1966; Webster 1972; Gill 1980) would give rise to an anticyclonic circulation to the east of the Philippines. Thus the area is affected by southerly winds resulting in decreased rainfall.

Overall the resemblance noted on the NDJF mean between the CS only and combined CS and MJO influences remain valid at the monthly time scale for all months albeit with more noise due to the reduced sampling and the rarity of combined CS and MJO days.

d. *Kinematic interaction between CSs and the MJO*

Besides the joint impact of CSs and the MJO on convection and rainfall, the interaction in the dynamic

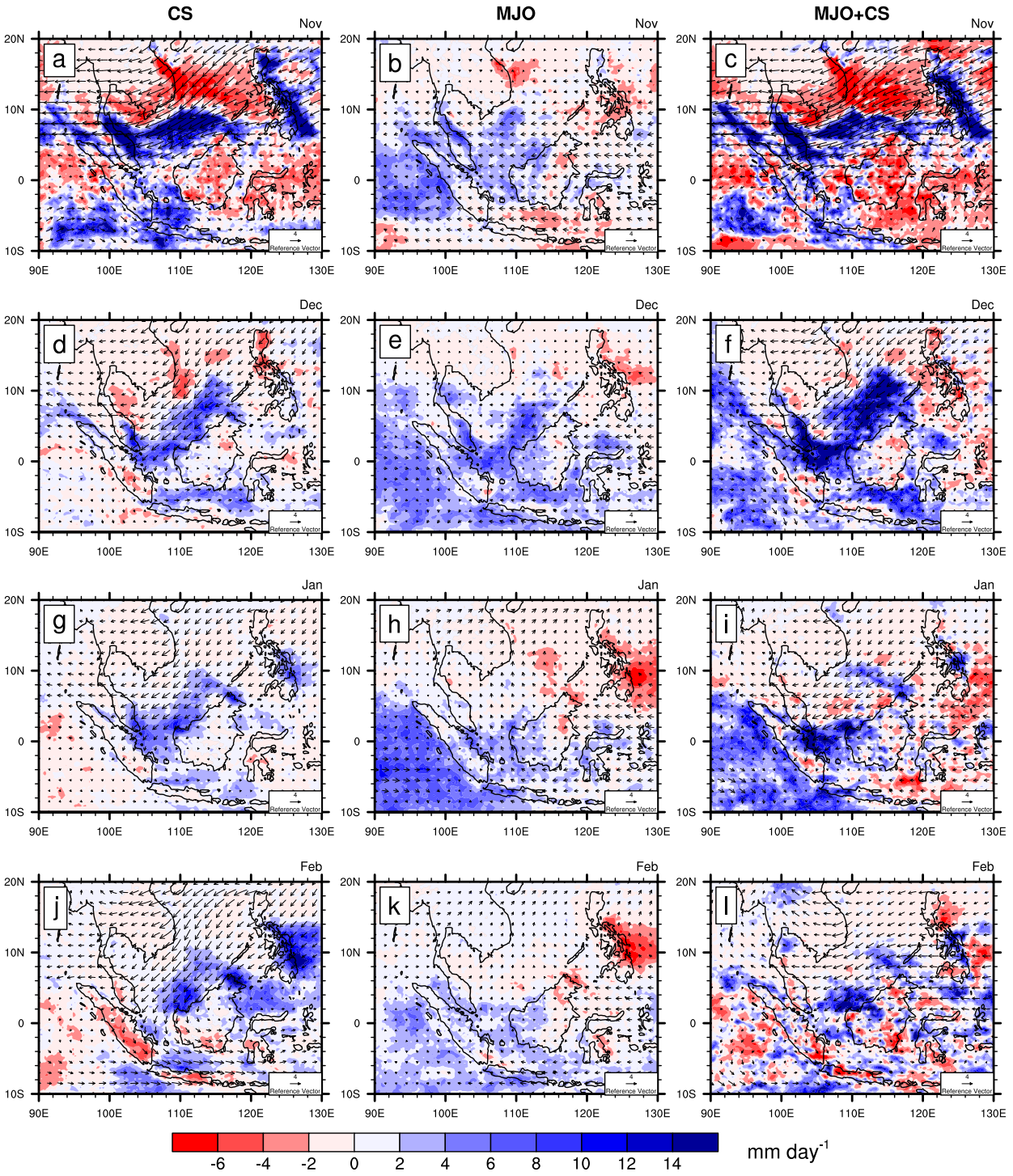

FIG. 10. Composites of monthly rainfall (shaded; mm day^{-1}) and wind speed (vectors; m s^{-1}) anomalies: (left) CS, (center) MJO, and (right) MJO+CS days for the months of (a)–(c) November, (d)–(f) December, (g)–(i) January, and (j)–(l) February.

structures of the two large-scale systems was analyzed by Chang et al. (2005a) using a singular value decomposition (SVD) analysis of the 30–60-day-bandpassed outgoing longwave radiation and zonal and 850-hPa meridional winds over an expanded Maritime Continent domain. During one-fourth of the oscillation when the Maritime Continent is under convectively suppressed condition, the associated anomalous circulation has significant

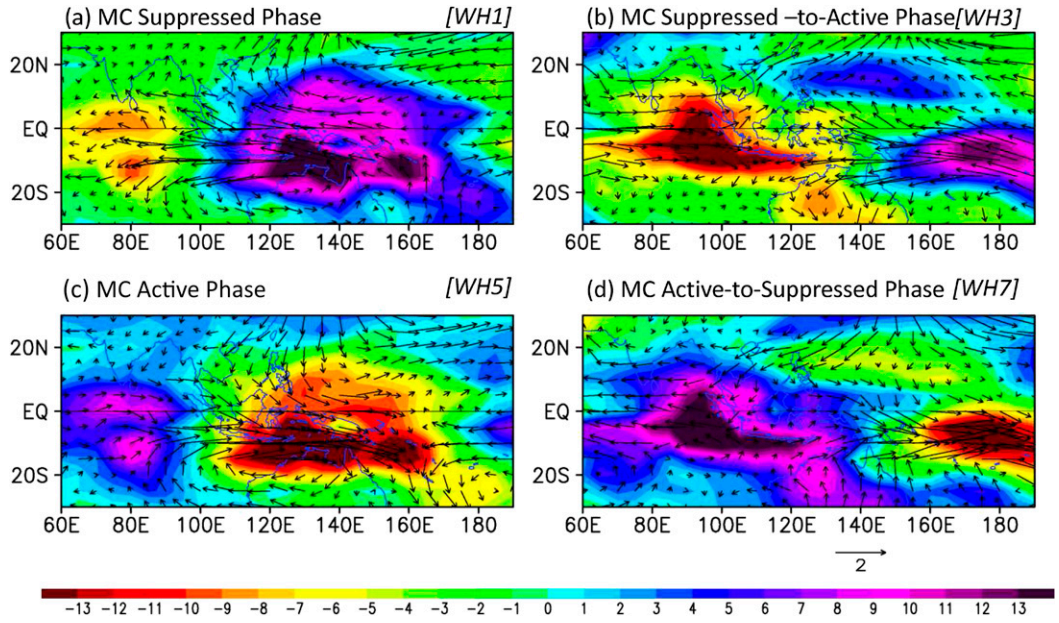

FIG. 11. Intraseasonal oscillation phases defined by SVD of OLR and 850-hPa winds over the expanded Maritime Continent domain. The corresponding RMM phases (Wheeler and Hendon 2004) are (a) 1, (b) 3, (c) 5, and (d) 7 [adapted from Chang et al. (2005a)].

southerly winds in the northern subtropics between 110° and 140°E [Fig. 11a, reproduced from Chang et al. (2005a)]. The development of these southerly anomalies may be related to Rossby wave response northwest of the area of suppressed condition. In the subsequent quarter cycle that represents the transition phase from suppressed to active condition (Fig. 11b), the southerly component expands markedly eastward to a much wider area reaching the date line. The entire SCS and the subtropical western North Pacific up to 150°E and beyond are occupied by an extensive belt of southwesterly winds that partially counter the northeast monsoon and CS winds. Chang et al. (2005a) found that during these two phases, which form one-half of the cycle, the frequency of CS is only 13% compared to 22% during the other half of the oscillation. There is also a corresponding decrease of Borneo vortex activity. They concluded that during the suppressed and the subsequent transition phases MJO inhibits cold surges and that weak surges are probably being more affected. The inhibition effect would be the largest during the suppressed-to-active transition phase because of the extensive southwesterly anomalies.

To confirm this, as the suppressed and the suppressed-to-active transition phases in Chang et al.'s (2005a) SVD analysis correspond closest to Wheeler and Hendon's (2004) phases 1 and 3, respectively, based on convective patterns, based on the chosen definition for the active MJO events (RMM phases 2–4) the frequency distribution of CS days in the 15 NDJF seasons for RMM phases 2–4 are compared to the other five phases (Table 5). When large MJO events are observed (RMM $\geq$ 1), the CS frequency for the active MJO (phases 2–4; 18.1%) is 25% less than the other phases confirming that active MJO does correspond to slightly reduced CS activity. The reduction is close to 17.5% if the weak MJO cases are included as a result of hardly any difference in CS frequency for weak MJO (Table 5, bottom). Furthermore, the addition of the w-S days (Table 5, right) reduces the frequency reductions as weaker surges are not affected by the MJO. We therefore confirm Chang et al.'s (2005a) findings that when MJO is active in SEA, which corresponds to the suppressed-to-active transition phase for the large Maritime Continent domain, CS activity is reduced, but the northeasterly flow is still strong and dominates the circulation over the SCS when both systems occur (Fig. 6c). In addition, this study indicates that this reduction effect is mainly on strong rather than weak surges.

5. Concluding remarks

Making use of the TRMM rainfall data from 1998 to 2012 combined with ERA-I, this study investigates the role of CS and MJO propagation either in isolation or combined in explaining rainfall anomalies (mean and extremes) across Southeast Asia during an extended period from November to February encompassing the NE monsoon affecting the region. It prolonged an earlier

study by Chang et al. (2005a), which focused on 1980–2001, and offered additional insights as the season of interest was extended to the month of November when CS are experienced, although the main NE monsoon flow is not usually established. Overall this new set of results is consistent with that prior study and in term of CS days and points to a small increase in the frequency of the CS events between the two periods. Although it is important to note that because of differences in methodology and datasets used, it may be entirely a result of methodological differences. Here, the definition of CSs is refined; northerly and northeasterly wind speeds and MSLP were considered in selecting the surge events, which occur in about 20%–25% of the days depending on whether a MSLP threshold is used. For the MJO the RMM from Wheeler and Hendon (2004) is used. All days during phases 2–4 with RMM amplitude equal to or larger than 1 are defined as active MJO days in the region.

CSs impact on rainfall are primarily driven by wind–terrain interaction: convergence produced by strong onshore winds against terrain over many parts of the region and enhanced shear vorticity strengthening the Borneo vortex, a prominent feature of the Asian winter monsoon. These two processes result in increased rainfall in three areas: a check mark pattern around the southern SCS, the southeastern Philippines, and the Java Sea. The TRMM rainfall analysis also reveals important details that were not discernible in the blackbody temperature results of Chang et al. (2005a). It shows that the enhanced convection associated with the strengthening Borneo vortex causes compensating decreases in rainfall to its northwest near southern Vietnam and that a forced sinking motion and drying develop off the southwestern coast of Sumatra during surges. Further studies of the interactions between the large-scale CS and MJO forcing and the Borneo vortex were left aside for more in-depth analysis of the local impact of the CS.

The rainfall anomalies associated with the MJO days are a region of positive rainfall anomalies over the equatorial eastern Indian Ocean west of Sumatra, which is an area sheltered by terrain from CS influences, and therefore differ from the CS impact on rainfall. There are two other areas with significant out-of-phase relationships: The first is the equatorial Indian Ocean, where the surge-forced sinking motion behind the Sumatra mountains suppresses rainfall in the middle of a broad area that is dominated by positive anomalies during MJO. The second is around the southeastern Philippines, where the northwest–southeast coastline produces heavy rainfall when onshore surge wind develops, while during MJO the southerly wind anomalies associated with the Rossby-type response of an anticyclonic circulation suppress rainfall. But, very importantly, across the southern SCS similar rainfall anomalies are noted in response to these two large-scale influences. Therefore, it is not surprising that the pattern of the rainfall anomalies when both are present resembles closely that of the cold surge (except over the equatorial Indian Ocean) with an important nonlinear additional effect across the southern South China Sea. It reveals that the MJO contributes to a more favorable environment for convection by moistening the environment. This moistening can cover most of the equatorial SCS. Besides the impact on mean rainfall, the impact of CS in triggering extreme rainfall is about twice as large as the contribution from the MJO, and the largest extreme rainfall events are obtained when both CS and MJO occur, which provides valuable information to help improve predictions of these high-impact extreme weather events.

In terms of dynamics, our results confirm Chang et al.'s (2005a) findings that the frequency of CS events is reduced during one-half of the MJO cycle when convection over the larger Maritime Continent domain is under suppressed and suppressed-to-active transition phases. During these periods the southwesterly anomalies occupy a wide area of East Asia and western North Pacific, consistent with the Rossby wave response to the MJO convection pattern, and partially counter the northeast CS winds. One notable difference is that Chang et al. (2005a) has speculated that the weaker surges may be most affected; our results indicate this in fact it is the stronger CS cases which are the most affected.

Acknowledgments. This collaborative research is supported and funded by the Centre for Climate Research Singapore, Meteorological Service Singapore (MSS). PX would like to thank MSS for funding a visiting scientist program during the course of this work, and the Met Office for funding a portion of his time through the Joint DECC/Defra Met Office Hadley Centre Climate Programme (GA01101). CPC would like to thank the World Meteorological Organization and the World Weather Research Programme for supporting his travel to attend the Workshop on Intraseasonal Processes and Prediction in the Maritime Continent in Singapore, during which the goal and strategy of this research was finalized. The authors thank Dr. Chris Gordon for his helpful suggestions and comments on the manuscript as well as three anonymous reviewers.

REFERENCES

Chang, C.-P., J. E. Erickson, and K. M. Lau, 1979: Northeasterly cold surges and near-equatorial disturbances over the winter MONEX area during December 1974. Part I: Synoptic aspects. *Mon. Wea. Rev.*, **107**, 812–829, doi:10.1175/1520-0493(1979)107<0812:NCSANE>2.0.CO;2.

——, P. A. Harr, and H. J. Chen, 2005a: Synoptic disturbances over the equatorial South China Sea and western Maritime Continent during boreal winter. *Mon. Wea. Rev.*, **133**, 489–503, doi:10.1175/MWR-2868.1.

——, Z. Wang, J. McBride, and C. H. Liu, 2005b: Annual cycle of Southeast Asia—Maritime Continent rainfall and the asymmetric monsoon transition. *J. Climate*, **18**, 287–301, doi:10.1175/JCLI-3257.1.

——, ——, and H. Hendon, 2006: The Asian winter monsoon. *The Asian Monsoon*, B. Wang, Ed., Praxis, 89–127.

——, M. M. Lu, and H. Lim, 2016: Monsoon convection in the Maritime Continent: Interaction of large-scale motion and complex terrain. *Multiscale Convection-Coupled Systems in the Tropics: A Tribute to Dr. Michio Yanai*, *Meteor. Monogr.*, No. 56, Amer. Meteor. Soc., 6.1–6.29 doi:10.1175/AMSMONOGRAPHS-D-15-0011.1.

Chu, P.-S., and S.-U. Park, 1984: Regional circulation characteristics associated with a cold surge event over East Asia during winter MONEX. *Mon. Wea. Rev.*, **112**, 955–965, doi:10.1175/1520-0493(1984)112<0955:RCCAWA>2.0.CO;2.

Dee, D., and Coauthors, 2011: The ERA-Interim reanalysis: Configuration and performance of the data assimilation system. *Quart. J. Roy. Meteor. Soc.*, **137**, 553–597, doi:10.1002/qj.828.

Ding, Y. H., 1990: Build-up, air mass transformation and propagation of Siberian high and its relations to cold surge in East Asia. *Meteor. Atmos. Phys.*, **44**, 281–292, doi:10.1007/BF01026822.

Gill, A. E., 1980: Some simple solutions for heat-induced tropical circulation. *Quart. J. Roy. Meteor. Soc.*, **449**, 447–462, doi:10.1002/qj.49710644905.

Huffman, G. J., and Coauthors, 2007: The TRMM Multisatellite Precipitation Analysis (TMPA): Quasi-global, multiyear, combined-sensor precipitation estimates at fine scales. *J. Hydrometeor.*, **8**, 38–55, doi:10.1175/JHM560.1.

Johnson, R. H., and R. A. House, 1987: Precipitating cloud systems of the Asian monsoon. *Monsoon Meteorology*, C.-P. Chang and T. N. Krishnamurti, Eds., Oxford University Press, 298–353.

——, and C. P. Chang, 2007: Winter MONEX: A quarter-century and beyond. *Bull. Amer. Meteor. Soc.*, **88**, 385–388, doi:10.1175/BAMS-88-3-385.

Jones, C., D. E. Waliser, K. Lau, and W. Stern, 2004: Global occurrences of extreme precipitation and the Madden–Julian oscillation: Observations and predictability. *J. Climate*, **17**, 4575–4589, doi:10.1175/3238.1.

Madden, R. A., and P. R. Julian, 1994: Observations of the 40–50-day tropical oscillation—A review. *Mon. Wea. Rev.*, **122**, 814–837, doi:10.1175/1520-0493(1994)122<0814:OOTDTO>2.0.CO;2.

Matsuno, T., 1966: Quasi-geostrophic motions in the equatorial area. *J. Meteor. Soc. Japan*, **43**, 25–43.

Meteorological Service Singapore, 2015: Annual climate assessment 2015. Centre for Climate Research Singapore Rep., 16 pp. [Available online at http://www.weather.gov.sg/wp-content/uploads/2016/03/Annual-Climate-Assessment-Report-2015.pdf.]

Moten, S., F. Yunus, M. Ariffin, N. Burham, D. J. Yik, M. K. M. Adam, and Y. W. Sang, 2014: Statistics of northeast monsoon onset, withdrawal and cold surges in Malaysia. Malaysian Meteorological Dept. Tech. Rep., 27 pp. [Available online at http://www.met.gov.my/in/web/metmalaysia/publications/technicalpaper/fullpapers/document/44759/rp00_2014.pdf.]

Peatman, S. C., A. J. Matthews, and D. J. Stevens, 2014: Propagation of the Madden–Julian oscillation through the Maritime Continent and scale interaction with the diurnal cycle of precipitation. *Quart. J. Roy. Meteor. Soc.*, **140**, 814–825, doi:10.1002/qj.2161.

Pullen, J., A. L. Gordon, M. Flatau, J. D. Doyle, C. Villanoy, and O. Cabrera, 2015: Multiscale influences on extreme winter rainfall in the Philippines. *J. Geophys. Res. Atmos.*, **120**, 3292–3309, doi:10.1002/2014JD022645.

Ramage, C. S., 1971: *Monsoon Meteorology*. International Geophysics Series, Vol. 15, Academic Press, 296 pp.

Reynolds, R. W., T. M. Smith, C. Liu, D. B. Chelton, K. S. Casey, and M. G. Schlax, 2007: Daily high-resolution-blended analyses for sea surface temperature. *J. Climate*, **20**, 5473–5496, doi:10.1175/2007JCLI1824.1.

Tangang, F. T., L. Juneng, E. Salimun, P. N. Vinayachandran, K. S. Yap, C. J. C. Reason, S. K. Behera, and T. Yasunari, 2008: On the roles of the northeast cold surge, the Borneo vortex, the Madden–Julian oscillation, and the Indian Ocean dipole during the extreme 2006/2007 flood in southern Peninsular Malaysia. *Geophys. Res. Lett.*, **35**, L14S07, doi:10.1029/2008GL033429.

Webster, P. J., 1972: Response of the tropical atmosphere to local steady forcing. *Mon. Wea. Rev.*, **100**, 518–541, doi:10.1175/1520-0493(1972)100<0518:ROTTAT>2.3.CO;2.

Wheeler, M. C., and H. H. Hendon, 2004: An all-season real-time multivariate MJO index: Development of an index for monitoring and prediction. *Mon. Wea. Rev.*, **132**, 1917–1932, doi:10.1175/1520-0493(2004)132<1917:AARMMI>2.0.CO;2.

Wongsaming, P., and R. H. B. Exell, 2011: Criteria for forecasting cold surges associated with strong high pressure areas over Thailand during the winter monsoon. *J. Sustainable Energy Environ.*, **2**, 145–156.

Wu, M., and J. C. Chan, 1995: Surface features of winter monsoon surges over south China. *Mon. Wea. Rev.*, **123**, 662–680, doi:10.1175/1520-0493(1995)123<0662:SFOWMS>2.0.CO;2.

Wu, P., M. Hara, H. Fudeyasu, M. D. Yamanaka, J. Matsumoto, F. Syamsudin, R. Sulistyowati, and Y. S. Djajadihardja, 2007: The impact of trans-equatorial monsoon flow on the formation of repeated torrential rains over Java Island. *SOLA*, **3**, 93–96, doi:10.2151/sola.2007-024.

Xavier, P., R. Rahmat, W. K. Cheong, and E. Wallace, 2014: Influence of Madden–Julian oscillation on Southeast Asia rainfall extremes: Observations and predictability. *Geophys. Res. Lett.*, **41**, 4406–4412, doi:10.1002/2014GL060241.